

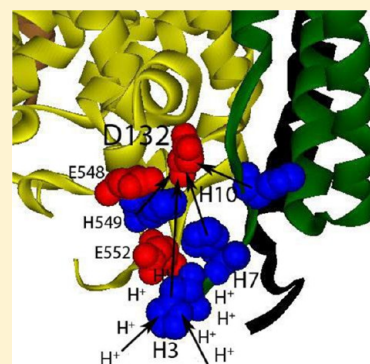
# Role of the N-Terminus of Subunit III in Proton Uptake in Cytochrome *c* Oxidase of *Rhodobacter sphaeroides*

Khadijeh S. Alnajjar,<sup>†</sup> Jonathan Hosler,<sup>‡</sup> and Lawrence Prochaska<sup>\*,†</sup>

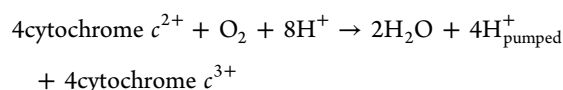
<sup>†</sup>Department of Biochemistry and Molecular Biology, Boonshoft School of Medicine, Wright State University, Dayton, Ohio 45435, United States

<sup>‡</sup>Department of Biochemistry, University of Mississippi Medical Center, Jackson, Mississippi 39216, United States

**ABSTRACT:** The catalytic core of cytochrome *c* oxidase consists of three subunits that are conserved across species. The N-terminus of subunit III contains three histidine residues (3, 7, and 10) that are surface-exposed, have physiologically relevant pK<sub>a</sub> values, and are in close proximity of the mouth of the D-channel in subunit I. A triple-histidine mutation (to glutamine) was created in *Rhodobacter sphaeroides*. The mutant enzyme retains 60% of wild-type activity. Absorbance during steady-state turnover indicates that electrons accumulate at heme *a* in the mutant, accompanied by accumulation of the oxoferryl intermediate. When reconstituted into liposomes, the mutant enzyme pumps protons with an efficiency that is half that of the wild type. Finally, the mutant exhibits a lower cytochrome *c* peroxidation rate. Our results indicate that the mutation lowers activity indirectly by slowing the uptake of protons through the D-channel and that the three histidine residues stabilize the interactions between subunit I and subunit III.



Cytochrome *c* oxidase (COX) is the terminal complex of the electron transport chain in mitochondria. It accepts electrons from cytochrome *c* and, in turn, reduces molecular oxygen to produce two water molecules while pumping one proton per electron transferred.<sup>1</sup> The reaction is summarized in the following equation:



During a single catalytic turnover, electrons are transferred sequentially from cytochrome *c* through Cu<sub>A</sub> (in subunit II) and heme *a* to the binuclear center in subunit I (SUI) (Figure 1, yellow). Molecular oxygen binds at the binuclear center, comprised of heme *a*<sub>3</sub> and Cu<sub>B</sub>, and is reduced to form water. In concert with electron transfer, four protons are transferred from the mitochondrial matrix to the binuclear center for water production (chemical protons) while four other protons are pumped across the membrane.<sup>2,3</sup> The first two chemical protons are transferred through the K-channel, named after a conserved K362 in SUI,<sup>4</sup> while the two remaining chemical protons and all pumped protons are transferred through the D-channel, named after a conserved D132 in SUI.<sup>4</sup> The K-channel originates at E101 in subunit II (SUII) and terminates at Y288 in SUI. The D-channel originates at D132 in SUI and is connected by a chain of resolved water molecules to form a channel to E286, which is located 10 Å from the binuclear center.<sup>4–6</sup> It has been suggested that E286 is the site at which protons are directed to either the binuclear center or the pump-loading site.<sup>7,8</sup> The pump-loading site is proposed to be the D-propionate group of heme *a*<sub>3</sub> along with a closely associated

arginine residue (R481) in SUI, but this has not been fully resolved.<sup>9–11</sup>

Subunit III (SUIII) of the catalytic core, containing a highly conserved amino acid sequence from prokaryotes to eukaryotes, is positioned adjacent to SUI.<sup>4</sup> It has seven transmembrane  $\alpha$ -helices organized into two bundles that form a V-shaped cleft with the N-terminus in the proximity of the mouth of the D-channel of SUI.

The removal of SUIII from the enzyme using nonionic detergents caused a decrease in proton pumping efficiency and resulted in turnover-induced suicide inactivation.<sup>12</sup> This phenomenon occurs by an unknown mechanism during the reduction of molecular oxygen and ultimately leads to the loss of Cu<sub>B</sub>.<sup>12,13</sup> I–II oxidase has a lowered heme *a*<sub>3</sub> reduction potential, suggesting a lack of proton transfer to the active site, which would otherwise neutralize the charge caused by electron transfer and increase the reduction potential of heme *a*<sub>3</sub>.<sup>13</sup> Additionally, the pK<sub>a</sub> of steady-state electron transfer activity decreases to 7.3 when SUIII is removed as compared to that of the wild-type enzyme (WT), which has a pK<sub>a</sub> of 8.5.<sup>14,15</sup>

Previous studies suggested that the protonation of D132 in the D-channel becomes the rate-limiting step in proton uptake during steady-state activity when SUIII is removed.<sup>15</sup> The mouth of the D-channel in SUI, D132, is protected from direct solvent exposure by a number of hydrophobic residues in SUI and SUIII such as P131 and P136 (SUI) and I11 and L12 (SUIII). This increases the pK<sub>a</sub> of D132, which maintains high rates of transfer of protons to the active site at higher pH

**Received:** November 15, 2013

**Revised:** January 2, 2014

**Published:** January 3, 2014



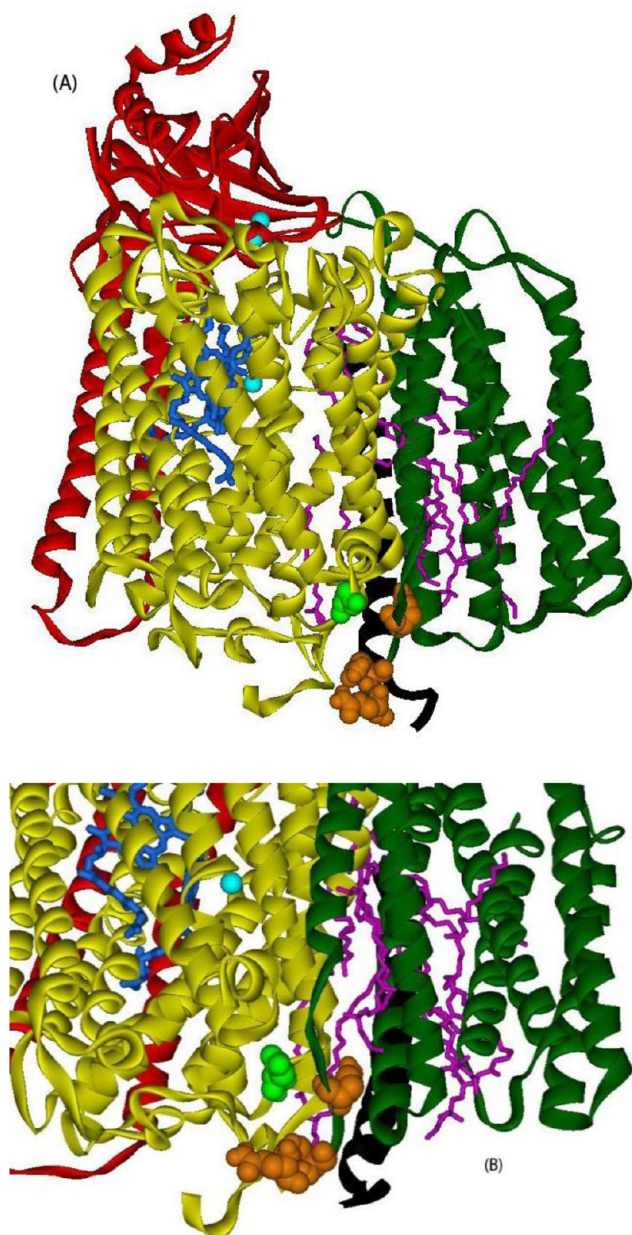


**Figure 1.** Three-dimensional model of the triple-histidine mutation in the N-terminus of subunit III of cytochrome *c* oxidase from *Rhodobacter sphaeroides*. (A) Subunit I (yellow) contains heme *a* and *a*<sub>3</sub> (blue), Cu<sub>B</sub> (cyan spheres). Subunit II (red) contains a bimolecular Cu<sub>A</sub> center (cyan spheres). Subunit III (green) contains phosphatidylethanolamine molecules (magenta). Subunit IV is colored black. The three mutated histidine residues (orange), shown near the N-terminus of SUIII, are each located within 12 Å of D132 (lime green), the initial proton acceptor of the D-channel. Coordinates from the three-dimensional structure of the crystallized wild-type COX (PDB entry 1M56 from ref 4) were used in Swiss protein data bank viewer (SPDBV) to model the mutation. The area located within 15 Å of histidine 10 was selected, and energy minimization was performed under steepest descent conditions with 2000 iterations. The mutated structure shows no significant differences from the wild type. (B) Close-up showing the proximity of the H3Q/H7Q/H10Q triple mutation (orange) to D132 (lime green).

values.<sup>16</sup> For example, at pH 9.0, the rate of proton uptake through the D-channel in the WT is  $\sim 10000 \text{ s}^{-1}$  during a single turnover.<sup>6,16–20</sup> These studies assume that there is a rapid

equilibrium between the N-side of the membrane and E286 and that the rate of transfer of a proton from E286 to the binuclear center is rate-limiting.<sup>6</sup> At the same pH, the rate of proton uptake through the D-channel by I–II oxidase decreases to  $350 \text{ s}^{-1}$ , which suggests that the rate-limiting step has changed and the rapid equilibrium across the D-channel to E286 does not exist.<sup>16</sup> Therefore, SUIII is essential for maintaining efficient proton uptake at higher pH values by providing a proton antenna near the D-channel.<sup>6</sup>

At pH >7, proton uptake in COX has been shown to occur at a rate as fast as  $100 \mu\text{s}$ , whereas the time constant for proton binding when it is limited by diffusion is  $\sim 1 \text{ ms}$ .<sup>20,21</sup> With a high rate of enzyme turnover, COX is not limited by proton diffusion at high pH. This suggests that buffering groups are necessary at the surface of the proton uptake channel not only to bind free protons at a high rate but also to retain them for immediate transfer at a rate determined by the rate of enzyme turnover and independent of proton diffusion.<sup>21</sup>

The N-terminus of SUIII contains three conserved histidine residues (3, 7 and 10), which are surface-exposed and are in the proximity ( $\sim 10 \text{ Å}$ ) of the mouth of the D-channel, D132. This suggests that the N-terminus of SUIII could act as a proton-collecting antenna to facilitate uptake of protons into the D-channel.<sup>14,16</sup> Additionally, these residues may contribute to the high buffering capacity of the N-side of the enzyme as determined by fluorescence studies.<sup>21,22</sup>

To investigate the role of these residues, we constructed a mutant form of *Rhodobacter sphaeroides* COX in which all three of the conserved histidine residues were altered to glutamine (H3Q, H7Q, and H10Q). Electron transfer and proton translocating activities of the purified mutant enzyme were tested to show that, in the absence of the three histidine residues, oxygen reduction activity decreases with an accompanying increase in the reduction level of heme *a* and an increase in the extent of accumulation of the oxoferryl intermediate during steady-state activity. Taken together, these results elucidate the importance of the N-terminus of SUIII as a portion of a proton antenna acting as a site at which protons are stored for immediate proton uptake through the D-channel.

## MATERIALS AND METHODS

### Expression and Purification of Cytochrome *c* Oxidase.

Wild-type cytochrome *c* oxidase was expressed in *R. sphaeroides* with a polyhistidine tag on the N-terminus of SUI as previously reported.<sup>23</sup> A plasmid containing the mutant histidine (H3Q/H7Q/H10Q) in SUIII was prepared as described by Bratton et al.<sup>24</sup> Colonies of *R. sphaeroides* were grown under aerobic and dark conditions at  $32^\circ\text{C}$  in Sistrom medium to an optical density of 1.0–1.2 as described by Zhen et al.<sup>23</sup> Cells were collected by centrifugation, and crude membranes were separated by ultracentrifugation after solubilization in dodecyl maltoside (DM) as described by Hosler et al.<sup>25</sup> Cytochrome *c* oxidase was purified from the detergent-solubilized pellets using affinity chromatography on a Ni<sup>2+</sup>-NTA column. The enzyme was eluted from the column with excess histidine (100 mM), washed, and concentrated by ultrafiltration using 10 mM Tris, 40 mM KCl, and 0.1% DM (pH 8.0). Further purification was performed on ion exchange fast protein liquid chromatography (FPLC) using DEAE-SPW as the resin as described by Zhen et al.<sup>23</sup> Cytochrome *c* oxidase fractions were collected, and the concentration was determined spectrophotometrically by using the reduced minus oxidized spectra ( $\Delta\epsilon_{606-630} = 28.9 \text{ mM}^{-1} \text{ cm}^{-1}$ ).<sup>26</sup> The enzyme was analyzed for purity using SDS–



PAGE, absorbance spectroscopy, and electron transfer activity.<sup>27</sup>

**Two-Dimensional Gel Electrophoresis.** Seven micrograms of each sample was loaded on a 4 to 15% gradient Tris-HCl polyacrylamide gel supplied by Bio-Rad at pH 8.8, and electrophoresis was performed using a discontinuous buffer system consistent with that described by Schagger and von Jagow.<sup>28</sup> The resultant separated bands were cut and transferred to a sodium dodecyl sulfate gel containing 6 M urea using the method described by Fuller et al.<sup>29</sup> to identify the subunit content of the native complexes occurring in solution. The gels were stained with Coomassie Blue, and the band intensity was quantified by measuring pixels per unit area using Multi Gauge.

**Removal of Subunit III.** Subunit III was removed with the modified method of Bratton et al.<sup>13</sup> Briefly, the enzyme was incubated in 20 mM Tris, 150 mM KCl, and Triton X-100 at a concentration of 100 mg/mg of COX (~12%) for 30 min at 4 °C. The mixture was purified over a Ni<sup>2+</sup>-NTA column, and residual Triton-X 100 was washed away using 10 mM Tris, 40 mM KCl, and 0.1% DM (pH 8.0). COX fractions were collected, and the procedure was repeated to achieve nearly complete removal of SUIII.

**Steady-State Oxygen Reduction Activity.** COX activity was measured polarographically using a Clark-type oxygen electrode in the appropriate buffer in the presence of 0.1% DM, 20  $\mu$ M cytochrome *c*, 17 mM ascorbic acid, and 0.6 mM TMPD. The pH dependence of oxygen reduction was measured in the appropriate buffer (MES for pH 6.5, HEPES for pH 7.0–8.5, and CHES for pH 9.0–10.0) at a constant ionic strength (*I* = 100 mM) in the presence of 0.1% DM. The effect of zinc on activity was studied by incubating the enzyme with 200  $\mu$ M ZnSO<sub>4</sub> for 15–30 min and measuring steady-state oxygen reduction activity in 50 mM potassium phosphate and 0.05% DM (pH 7.4) in the presence of 200  $\mu$ M ZnSO<sub>4</sub>.

**Steady-State Peroxidase Activity.** Cytochrome *c* peroxidase activity was measured at 550 nm ( $\epsilon_{550}$  = 29.5 mM<sup>-1</sup> cm<sup>-1</sup>)<sup>30</sup> as the rate of ferrocyanochrome *c* oxidation using a Hewlett-Packard UV/visible diode array spectrophotometer. The reduction of 25 mM hydrogen peroxide in the presence of 5  $\mu$ M ferrocyanochrome *c* was initiated by the addition of 1 nM COX in 25 mM CHES and 0.1% DM (pH 10.0).<sup>31</sup>

**Heme *a* Reduction Level.** Heme *a* reduction levels of cytochrome *c* oxidase (0.3  $\mu$ M) were monitored spectrophotometrically at 444–460 and 604–650 nm in the presence of 1 mM ascorbate and 100  $\mu$ M TMPD in 25 mM CHES (pH 9.5) with 0.1% DM at a constant ionic strength (*I* = 100 mM). Spectra of the initial oxidized species were recorded during steady-state turnover for 5 min, and spectra of the fully reduced species were also recorded. Data were normalized to the absorbance of the fully reduced enzyme after subtracting the contribution of the oxidized heme for comparison. Additionally, data were corrected for baseline in the  $\alpha$ -region. Heme reduction was calculated as the ratio of the absorbance 5 min after steady-state activity had been initiated compared to the fully reduced state.<sup>31,32</sup>

**Proton Pumping.** Cytochrome *c* oxidase was preincubated with 3 mg Triton X-100/mg of COX for 15 min at 4 °C. Asolectin (phosphatidylcholine from Sigma) at 40 mg/mL was sonicated in the presence of 100 mM Hepes (pH 7.2) and 2.5% cholate until the solution became clear. The preincubated enzyme was mixed with sonicated asolectin at 4  $\mu$ M and dialyzed against 50  $\mu$ M Hepes, 50 mM sucrose, and 50 mM

KCl (pH 7.2) overnight at 4 °C to remove excess detergent.<sup>27</sup> Proton pumping was measured using an SX.18MV Applied Photophysics stopped-flow spectrophotometer at 558 nm in the presence of 100  $\mu$ M phenol red as a pH indicator dye. The reaction was initiated by rapidly mixing 2  $\mu$ M ferrocyanochrome *c* with 0.1  $\mu$ M COX in 50  $\mu$ M Hepes, 50 mM sucrose, and 50 mM KCl (pH 7.4). To measure proton pumping efficiency, absorbance changes of phenol red were measured in the presence of 5  $\mu$ M valinomycin (controlled conditions) or in the presence of both 5  $\mu$ M valinomycin and 5  $\mu$ M CCCP (uncontrolled condition). Traces were corrected for absorbance changes resulting from liposomes in the absence of COX. The respiratory control ratio (RCR), which is an indicator of the permeability of the liposomes, and electron transfer activity rates were measured as described previously.<sup>27</sup>

## RESULTS

An altered form of the COX in which histidines 3, 7, and 10 of SUIII were mutated to glutamine was expressed in *R. sphaeroides*. The histidine-tagged mutant enzyme (TM) was purified using nickel affinity chromatography and ion exchange FPLC. Limited molecular modeling of the mutations showed no significant structural effect on the surrounding region (Figure 1); therefore, the effects of the mutation on activity are not a result of altered structure.

**Histidines 3, 7, and 10 Are Important for the Association between Subunit I and Subunit III.** The mutation caused a partial dissociation of SUIII from the enzyme during purification by nickel affinity chromatography as shown by native gel electrophoresis and subsequent SDS-PAGE (Figure 2A,B). The gel shows that approximately one-half of the mutant enzyme lost SUIII after purification on the nickel column as quantified by the staining intensity of band 1 and band 2 (Figure 2A). The nickel-purified mutant enzyme was further chromatographed using ion exchange FPLC, and fractions containing SUIII were pooled with half the final yield of WT. Figure 2C shows the FPLC-purified mutant retains SUIII (lanes 2 and 4 for the FPLC-purified WT and TM, respectively).

**Steady-State O<sub>2</sub> Reduction Activity and pH Dependence.** Maximal rates of oxygen reduction were 40% slower in the mutant than in the WT at pH 7.4; however, the mutant exhibits a pH dependence of O<sub>2</sub> reduction activity similar to that of the WT with pK<sub>a</sub> values of 8.9 for the WT and 8.7 for the TM (Figure 3). This indicates that the mutations are slowing proton uptake; however, the rate is still faster than the rate-limiting step in proton uptake. Therefore, the pK<sub>a</sub> of steady-state activity did not change as a result of the mutations. In contrast, the steady-state activity of I–II oxidase exhibits a pK<sub>a</sub> of 7.3, because of the altered pH dependence of D-channel proton uptake in the absence of SUIII.<sup>16,33</sup>

Additionally, it has been shown that the presence of zinc slows the proton uptake reaction in COX, thereby decreasing steady-state activity possibly by coordinating with residues on the N-side of the enzyme.<sup>14,34,35</sup> The activity of the mutant in the presence of 200  $\mu$ M ZnSO<sub>4</sub> does not change significantly compared to that of the WT, which exhibits a 30% decrease in activity in the presence of zinc (Table 1). The mutant also exhibits behavior similar to that of zinc that is observed in I–II oxidase. This confirms that either all three of the histidine residues or any combination contributes to the coordination site of zinc in inhibiting the activity of cytochrome *c* oxidase.<sup>36–38</sup>

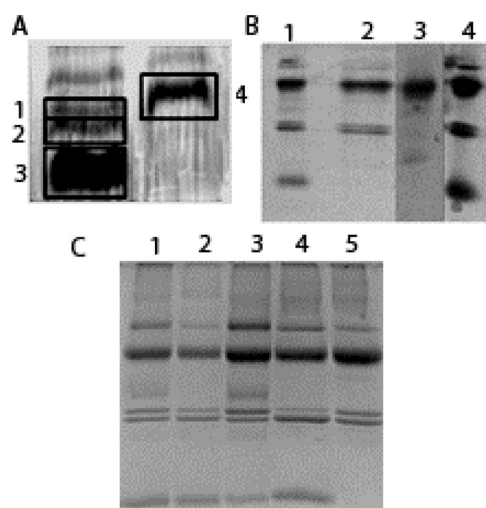


**Figure 2.** Gel electrophoresis of nickel-purified and FPLC-purified wild-type (WT) and triple-histidine mutant (TM) COX. (A) One-dimensional native gel, in which lane 1 contained the nickel-purified triple-histidine mutant and lane 2 the WT. (B) The two-dimensional gel was run under SDS denaturing conditions. Each lane in the second dimension corresponded to the respective number-labeled band in the first dimension (panel A). Lanes 1–3 show bands from the triple-histidine mutant, and lane 4 shows that from the WT. (C) SDS-PAGE comparing Ni<sup>2+</sup>-purified WT (lane 1), FPLC pure WT (lane 2), Ni<sup>2+</sup> pure TM (lane 3), FPLC pure TM (lane 4), and Ni<sup>2+</sup> pure I–II oxidase (lane 5). The double band for SUII shown in panels B and C is a result of post-translational proteolytic processing, which cleaves 25 amino acids in the N-terminus and 15 amino acids in the C-terminus as has been shown by Distler et al.<sup>58</sup>

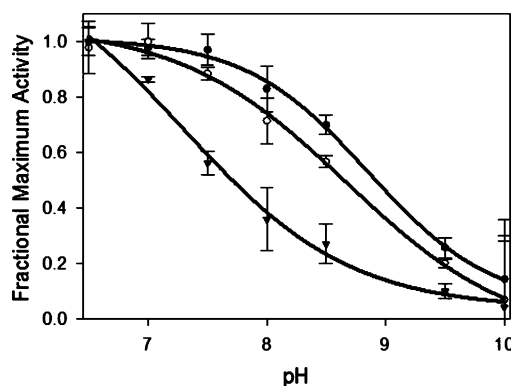


**Figure 3.** pH dependence of electron transfer activity of the WT, TM, and I–II COX. pH dependence of electron transfer activity plotted as the fractional maximal activity. Data points were fit with a single pK<sub>a</sub> three-parameter sigmoidal equation, in Sigma Plot, giving apparent pK<sub>a</sub> values of 8.85 ± 0.1, 8.67 ± 0.19, and 7.29 ± 0.35 for the wild type (●), the triple-histidine mutant (○), and I–II oxidase (▼), respectively.

**Table 1. Effect of Zinc Binding on Steady-State O<sub>2</sub> Reduction Activity**

	wild type	histidine mutant	I–II oxidase
activity <sup>a</sup>	1200 ± 10	700 ± 30	500 ± 20
activity with Zn <sup>b</sup>	830 ± 70	620 ± 10	450 ± 15

<sup>a</sup>Oxygen reduction activity measured in 50 mM potassium phosphate (pH 7.4) in the presence of 0.05% DM. Units are expressed in terms of electrons transferred per second. <sup>b</sup>Activity measured in the presence of 200 μM ZnSO<sub>4</sub>.

## Hydrogen Peroxide Reduction Shows That the Histidine Residues Are Important for the Uptake of Protons by the D-Channel.

Cytochrome *c* peroxidase activity was studied to specify the effect of the mutations on the D-channel proton uptake during steady-state activity. The addition of hydrogen peroxide increases the rate of cytochrome *c* oxidation at pH 10 because the reduction of hydrogen peroxide to water at the active site eliminates the need for K-channel protons.<sup>39–41</sup> Therefore, protons are transferred solely through the D-channel, and oxygen reduction activity becomes independent of the rates of uptake of protons through the K-channel. As a result, peroxidase activity is used to measure the dependence of steady-state activity on the uptake of protons through the D-channel. Figure 4 shows the kinetics of

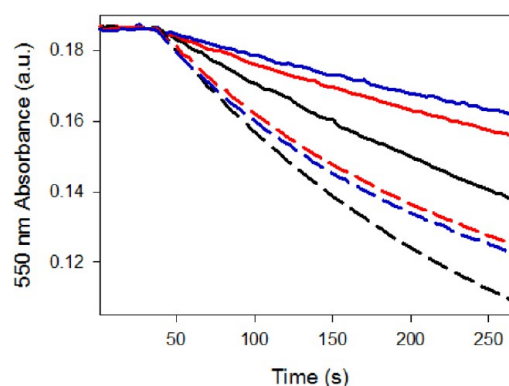


**Figure 4.** Cytochrome *c* peroxidase activity of the WT, TM, and I–II oxidase at pH 10. Cytochrome *c* oxidation rates in the absence (solid lines) and presence (dashed lines) of 25 mM hydrogen peroxide. The slope of the initial rate after the addition of 1 nM cytochrome *c* oxidase was used to determine turnover numbers of 6.8 ± 0.3, 4.1 ± 0.5, and 3.2 ± 0.5 μM cytochrome *c* s<sup>−1</sup> for the oxidase activity of the wild type (black), the triple-histidine mutant (red), and I–II oxidase (blue), respectively, and 14.2 ± 0.9, 9.4 ± 0.7, and 11.1 ± 0.2 μM cytochrome *c* s<sup>−1</sup> for the peroxidase activity of the wild type, the triple-histidine mutant, and I–II oxidase, respectively.

cytochrome *c* oxidation catalyzed by COX in the absence (solid lines) or presence (dashed lines) of hydrogen peroxide. These assays were conducted in high-pH buffer, pH 10, so that the peroxidase reaction predominates. The high-pH buffer was also used to observe the largest contrast between the WT and the mutant and to observe the largest effect of the antenna on activity.<sup>31,41</sup> The initial slope after the addition of COX was used to calculate rates of cytochrome *c* oxidation.

As expected, the rates of oxidase and peroxidase activities catalyzed by the mutant are slower than that of the WT by 40 and 35%, respectively. Both the mutant and WT COX exhibit an ~2-fold increase in the rates of cytochrome *c* oxidase when using hydrogen peroxide as a substrate (Table 2). This means that the mechanism by which the mutant lowers activity in the absence of hydrogen peroxide is the same as that in its presence, which can then be interpreted to be a delay in the delivery of protons specifically through the D-channel. Comparatively, the activity of I–II oxidase in the presence of hydrogen peroxide is 3.5-fold higher than in its absence, which means that the removal of SUIII has stronger effects on the activity in addition to having an effect on the D-channel.

**Delivery of Electrons to the Active Site Is Delayed as a Result of the Mutations in SUIII.** Electron transfer and proton uptake events are interdependent.<sup>42–44</sup> An initial

**Table 2. Cytochrome *c* Oxidation Activity in the Presence and Absence of Hydrogen Peroxide**

	wild type	histidine mutant	I–II oxidase
peroxidase activity <sup>a</sup>	14.2 ± 0.9	9.4 ± 0.7	11.1 ± 0.2
oxidase activity <sup>b</sup>	6.8 ± 0.3	4.1 ± 0.5	3.2 ± 0.5

<sup>a</sup>Activity measured in 25 mM CHES and 0.1% DM (pH 10.0) in the presence of 25 mM hydrogen peroxide and 5  $\mu$ M ferrocyanochrome *c*. Units are expressed in terms of micromolar cytochrome *c* oxidized per second. <sup>b</sup>In the absence of hydrogen peroxide. Units in terms of micromolar cytochrome *c* oxidized per second.

transfer of an electron to the active site is necessary to increase the  $pK_a$  of a nearby proton-accepting group. A subsequent proton transfer becomes essential for neutralizing the resultant negative charge, leading to an increase in the reduction potential of heme  $a_3$  and consequently increasing electron transfer rates.<sup>44</sup> Accordingly, a predicted delay in proton uptake is expected to decrease electron transfer rates from heme *a* to heme  $a_3$ . Electrons are therefore expected to accumulate at heme *a* during steady-state activity and result in decreased oxygen reduction rates. Figure 5 shows the heme absorbance in

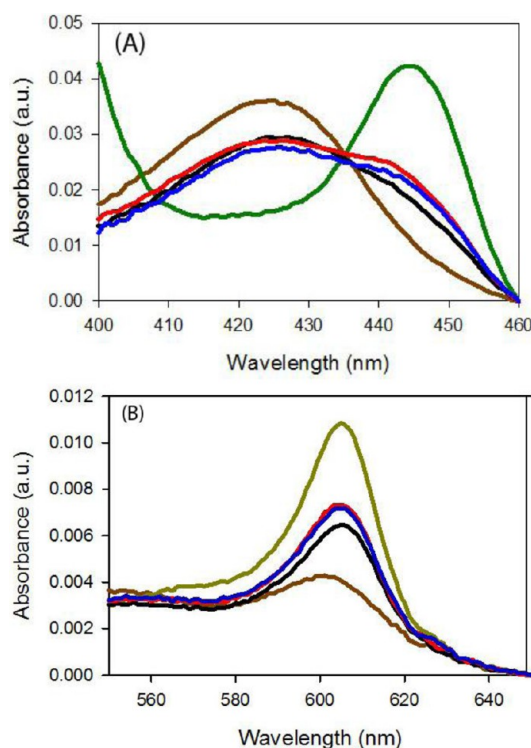


**Figure 5.** Steady-state heme *a* reduction levels of the WT, triple-histidine mutant, and I–II oxidase. The heme *a* reduction level during steady state was monitored at 444–460 nm (A) and 604–650 nm (B) at pH 9.5. The data for the WT during steady state are colored black, data for the TM red, and data for I–II oxidase blue. The oxidized spectrum is colored brown and the reduced spectrum green.

the Soret region (panel A) and  $\alpha$ -band (panel B) of the oxidized state, the steady state at pH 9.5, and the reduced state of the WT, mutant, and I–II oxidase. Heme *a* contributes 50% to the absorbance in the Soret region of the spectrum (Figure 5A) and 85% to the absorbance in the  $\alpha$ -peak (Figure 5B).<sup>45</sup> Our results show that  $18 \pm 2\%$  of both heme moieties of WT are reduced in the Soret region and  $36 \pm 3\%$  are reduced the  $\alpha$ -peak. Comparatively, the mutant shows a higher percent of

heme reduction,  $29 \pm 2\%$  in the Soret region and  $50 \pm 4\%$  in the  $\alpha$ -band, confirming that the histidine residues are indirectly slowing electron transfer by slowing the uptake of protons through the D-channel. I–II oxidase shows a reduction pattern of the heme similar to that of the mutant, which is another line of evidence that those residues are essential for oxygen reduction activity at pH 9.5.

Results from steady-state heme measurements also reveal that the oxoferryl intermediate accumulates at a faster rate in the mutant than in the WT, which is apparent in the formation of the  $A_{439}$  peak over time during steady state (Figure 6). The

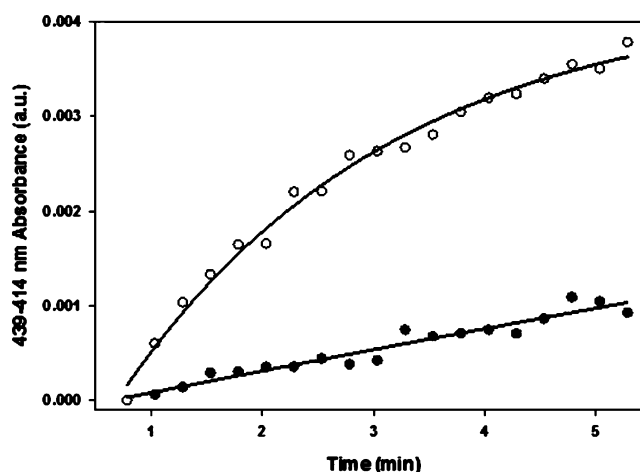


**Figure 6.** Formation of the  $A_{439}$  species as a function of time during the steady-state oxygen reduction activity of the WT and triple-histidine mutant. The triple-histidine mutant (O) accumulated 3.5-fold more of the  $A_{439}$  species after oxygen reduction for 5 min than the WT (●). Data were fit with a single-exponential rise to maximum curve with rates of  $0.35 \text{ mM s}^{-1}$  ( $\Delta\epsilon_{439-414} = 50.7 \text{ mM}^{-1} \text{ cm}^{-1}$ )<sup>26</sup> for the mutant and  $0.017 \text{ mM s}^{-1}$  for the WT.

mutant shows a 3.5-fold higher rate of accumulation of the  $A_{439}$  species after steady-state activity for 5 min, which appears at a rate of  $0.35 \pm 0.01 \text{ mM s}^{-1}$ ;<sup>26</sup> however, the WT showed minimal change in the absorbance at  $A_{439}$  over time (Figure 6).

**The Mutations in SUIII Lower the Proton Pumping Efficiency.** Figure 7 shows absorbance changes of phenol red when the rapid mixing of cytochrome *c* oxidase with cytochrome *c* was initiated as measured by the stopped-flow spectrophotometer. The proton pumping efficiency indicates the ability of the enzyme to capture the energy released from oxygen reduction to pump protons. The bottom red trace of Figure 7 shows that 50% of protons are pumped, which means that only 50% of the protons are delivered in time to capture the energy released from oxygen reduction compared to WT (black). A similar decrease in proton pumping efficiency also occurs when SUIII is removed.<sup>14</sup>

## DISCUSSION

Although SUIII is not necessary for oxygen reduction activity, timed electron transfer events and conservation of energy for efficient proton pumping require its presence.<sup>46–49</sup> SUIII is also necessary for an extended life span of the enzyme because of the increased probability for turnover-induced suicide inactivation in its absence.<sup>12,13,15</sup> The prevention of suicide inactivation has been linked to the ability of SUIII to maintain the rapid uptake of protons through the D-channel at high pH values.<sup>16,33</sup> Thus, SUIII is an important part of the catalytic



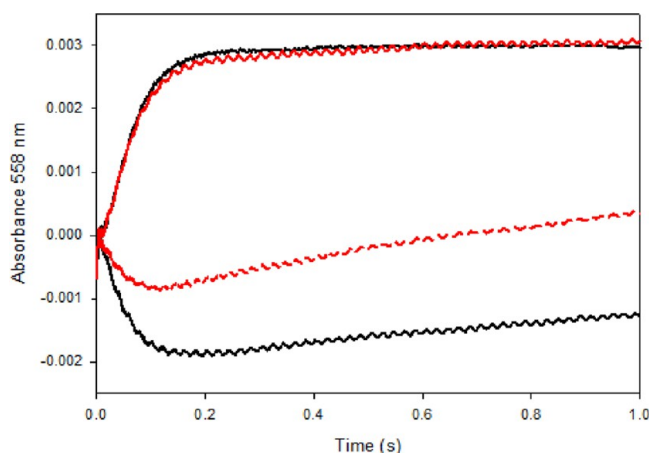


**Figure 7.** Proton pumping of wild-type COX and the triple-histidine mutant incorporated into liposomes. Proton pumping was measured by stopped-flow absorbance spectroscopy at 558 nm using 100  $\mu$ M phenol red as a pH indicator dye. Presented are average traces for five enzymatic turnovers. The  $H^+/e^-$  ratio is calculated from the extent of the maximal absorbance decrease from the bottom traces (black for the WT and red for the TM) (controlled conditions in the presence of 5  $\mu$ M valinomycin) divided by the maximal absorbance increase from the top traces (black for the WT and red for the TM) (uncontrolled conditions in the presence of 5  $\mu$ M valinomycin and 5  $\mu$ M CCCP). The WT exhibited a  $H^+/e^-$  ratio of  $0.68 \pm 0.21$  with an RCR of  $8.0 \pm 1.0$ , whereas the mutant showed a ratio of  $0.27 \pm 0.07$  and an RCR of  $4.5 \pm 1.3$ .

core of cytochrome *c* oxidase, even though it does not contain any metal centers. Subunit III has also been suggested to supply proton antenna residues that may enhance the uptake of protons into the D-channel,<sup>16,50</sup> but evidence supporting this hypothesis is incomplete. The purpose of this study is to determine if conserved histidine residues located in the N-terminus of SUIII facilitate the uptake of protons through the D-channel during steady-state activity.

H3, H7, and H10 on the N-terminus of SUIII are located near the mouth of the D-channel, D132 in SUI. Histidine residues have the ability to bind protons and act as a proton-collecting antenna.<sup>21,51</sup> They could create a proton reservoir at the entry point of a proton uptake pathway at a rate that is faster than the rate of diffusion from the bulk solvent.<sup>51</sup> Our results support the work of Adelroth and Brzezinski,<sup>50</sup> who concluded that an efficient proton collection antenna is best described as histidine residues surrounded by acidic groups located near a proton uptake channel. This permits rapid protonation from solution and the ability to reserve protons for proton uptake through the channel when needed.<sup>50</sup>

**Protection of the Mouth of the D-Channel by Weak Interactions between SUI and SUIII.** The first indicator that these three histidine residues are important for structure and function was the loss of SUIII during purification of the mutant by nickel affinity chromatography. FPLC purification eliminated most of I–II oxidase, though the loss of SUIII may occur during catalytic turnover.

The interaction energy between SUI and SUIII has been previously studied by differential scanning calorimetry in *Paracoccus denitrificans*,<sup>52</sup> and the data showed that SUIII undergoes thermal denaturation in a manner different from that of the rest of the enzyme at  $\sim 47^\circ\text{C}$  compared to I–II oxidase at  $67^\circ\text{C}$ . The histidine residues are located in the proximity of the C-terminus of SUI, which contains a number of charged

residues such as E548, H549, E552, K556, R557, E558, and D559. These residues can interact to form weak interactions with the histidine residues, preserving the integrity of the SUI–SUIII interface. Our mutation data are consistent with those of Varanasi and Hosler,<sup>53</sup> who showed that there was very weak binding of SUIII to SUI and the loss of any one interaction can lead to a large-scale loss of SUIII. Our results could mean that the removal of any of the three charged groups in SUIII weakens the SUI–SUIII interaction. Alternatively, these histidine residues could be important for the *in vivo* assembly of SUIII onto SUI.<sup>54</sup>

**Buffering Capacity of the N-Side of the Membrane.** A recent study by Kirchberg et al.<sup>22</sup> investigated the buffering capacity of the N-side of COX. This study shows that the amino acids located near the D-channel are able to buffer against small pH changes, making rates of uptake of protons through the D-channel independent of small changes in the pH of the surrounding environment. Though I–II oxidase was used in this study, the conclusion could be extrapolated to the WT because additional residues are likely involved in buffering and SUIII has an amino acid composition at the N-terminus similar to that of a typical proton antenna.<sup>21,51,55</sup> The H3Q/H7Q/H10Q mutant COX exhibits lower steady-state electron transfer activity without a change in its  $pK_a$  value (Figure 3). The retention of the WT  $pK_a$  suggests that the environment around D132 has not been altered and that SUIII remains present. Therefore, these histidine residues are likely acting as antenna residues as proposed by Gilderson et al.<sup>16</sup>

Our results show that the steady-state activity of the mutant is more inhibited at high pH ( $>7.5$ ) where a proton antenna would be essential because of the lack of bulk protons from the solution. This becomes relevant under physiological conditions where the pH of the mitochondrial matrix is higher, 7.9–8.0 depending on the cell type.<sup>56</sup> For example, the WT exhibits a 45% decrease in activity with half a pH unit increase at pH 9.5; however, the mutant exhibits a 60% decrease in activity. This suggests that the enzyme was able to buffer the environment surrounding the D-channel at low pH values but starts to lose this ability in the absence of the three histidine residues on SUIII at high pH values.<sup>51,55</sup>

Additionally, when COX is incorporated into liposomes, the interior pH increases during steady-state turnover because of the consumption of protons from the vesicle interior. When a proton ionophore (CCCP) is added, the pH across the membrane equilibrates. The data from Figure 7 show that the rate of coupled  $O_2$  reduction is slower in the mutant enzyme than in the WT. When CCCP is added, the proton concentration on the inside of liposomes equilibrates with that of the external buffer, at pH 7.4, and the rates of  $O_2$  reduction by both COX forms are similar.

**COX Turnover That Requires Only the D-Pathway Is Inhibited by the Removal of the Subunit III Histidine.** Previous studies have shown that the peroxidase activity of COX is independent of the K-channel and that at high pH values, peroxidase activity is greater than oxidase activity.<sup>41,57,58</sup> Upon comparison of rates of peroxidase and oxidase in both the WT and the mutant (Figure 4), the ratios of the WT and the mutant are approximately the same (2.3- and 2.1-fold increases, respectively, upon addition of hydrogen peroxide). Once SUIII is removed, the ratio of peroxidase to oxidase activity is greater than that of the WT. This suggests that the mechanism by which the mutation slows activity is the same whether hydrogen peroxide is absent or present and that the

mutation lowers activity by slowing the uptake of protons by the D-channel. It seems likely that  $H_2O_2$  can enter the active site more easily in the absence of the barrier imposed by SUIII.

A decrease in proton pumping efficiency (Figure 7) upon the introduction of the three histidine mutations provides additional support for the idea that these residues are essential for the rapid uptake of protons through the D-channel. The delivery of a proton to the proton loading site occurs only when E286 of the D-channel is in the correct configuration.<sup>20,21</sup> The decreased proton pumping efficiency seen in the mutant could be a result of a delay in the delivery of protons to the proton loading site when the configuration of the side chain of E286 is in the correct orientation.<sup>19,20</sup>

Finally, the effect of zinc on activity provides additional evidence showing that the mutant has difficulty taking up D-pathway protons. Muramoto et al.<sup>38</sup> showed by X-ray crystallography that a zinc molecule binds at a histidine residue located at the C-terminus of SUI, near the N-terminus of SUIII.<sup>38</sup> Our results support the idea that these residues are involved in the uptake of protons through the D-channel because proton uptake in the presence of Zn during a single turnover is delayed with an increasing concentration of Zn.<sup>20,36</sup> Our work demonstrates that one or all of the three histidine residues are required for Zn inhibition.

**The Transfer of Electrons from Heme  $a$  to Heme  $a_3$  Slows as a Result of Decreased Proton Uptake Rates.** The heme reduction assay shows that a modification of the enzyme causes either a direct or an indirect change in heme reduction levels during steady-state activity.<sup>31</sup> This implies that a change in proton uptake can indirectly slow the electron transfer pathway.<sup>42–44,57</sup> Therefore, our data suggest that the slower heme  $a$  to  $a_3$  electron transfer is consistent with slower D-pathway proton uptake.

Our conclusion that the mutation causes a delay in the uptake of protons through the D-channel was also supported by the accumulation of the  $A_{439}$  species (oxyferryl intermediate) over time during the steady state. This indicates that the uptake of protons through the D-channel is slowed, causing the  $A_{439}$  species to accumulate. In summary, our results show that one, two, or all three histidine residues in the N-terminus of SUIII are necessary to stabilize the interactions between SUI and SUIII and may play a role in facilitating the assembly of SUIII onto SUI. Additionally, this work shows that the N-terminus of SUIII of COX is important for the efficient uptake of protons into the D-channel at high pH values.

## AUTHOR INFORMATION

### Corresponding Author

\*E-mail: lawrence.prochaska@wright.edu. Phone: (937) 775-2551.

### Funding

Support was provided by the Wright State University Foundation in memory of Henry and Emily Webb and the Boonshoft School of Medicine of Wright State University. K.S.A. was supported by the Biomedical Sciences Ph.D. program at Wright State University.

### Notes

The authors declare no competing financial interest.

## ACKNOWLEDGMENTS

We thank Dr. Gerald Alter for his assistance in modeling the mutation using SPDBV.

## ABBREVIATIONS

CCCP, carbonylcyanide *m*-chlorophenylhydrazone; CHES, *N*-cyclohexyl-2-aminoethanesulfonic acid; COX, cytochrome *c* oxidase; DM, dodecyl maltoside; FPLC, fast protein liquid chromatography; HEPES, 4-(2-hydroxyethyl)-1-piperazineethanesulfonic acid; MES, 2-(*N*-morpholino)ethanesulfonic acid; NTA, nitrilotriacetic acid; PDB, Protein Data Bank; RCR, respiratory control ratio; SDS–PAGE, sodium dodecyl sulfate–polyacrylamide gel electrophoresis; SPDBV, Swiss Protein Data Bank Viewer; SUI, subunit I; SUII, subunit II; SUIII, subunit III; TM, triple-histidine mutant; TMPD, tetramethylphenylenediamine; WT, wild type.

## ADDITIONAL NOTE

<sup>a</sup>Amino acid residues are numbered according to the cytochrome *c* oxidase sequence from *R. sphaeroides* unless otherwise noted.

## REFERENCES

- (1) Wikstrom, M. K. (1977) Proton pump coupled to cytochrome *c* oxidase in mitochondria. *Nature* 266, 271–273.
- (2) Fetter, J. R., Qian, J., Shapleigh, J., Thomas, J. W., Garcia-Horsman, A., Schmidt, E., Hosler, J., Babcock, G. T., Gennis, R. B., and Ferguson-Miller, S. (1995) Possible proton relay pathways in cytochrome *c* oxidase. *Proc. Natl. Acad. Sci. U.S.A.* 92, 1604–1608.
- (3) Michel, H. (1998) The mechanism of proton pumping by cytochrome *c* oxidase. *Proc. Natl. Acad. Sci. U.S.A.* 95, 12819–12824.
- (4) Svensson-Ek, M., Abramson, J., Larsson, G., Tornroth, S., Brzezinski, P., and Iwata, S. (2002) The X-ray crystal structures of wild-type and EQ(I-286) mutant cytochrome *c* oxidases from *Rhodobacter sphaeroides*. *J. Mol. Biol.* 321, 329–339.
- (5) Namslaue, A., Lepp, H., Branden, M., Jasaitis, A., Verkhovsky, M. I., and Brzezinski, P. (2007) Plasticity of proton pathway structure and water coordination in cytochrome *c* oxidase. *J. Biol. Chem.* 282, 15148–15158.
- (6) Wikstrom, M., and Verkhovsky, M. I. (2011) The D-channel of cytochrome oxidase: An alternative view. *Biochim. Biophys. Acta* 1807, 1273–1278.
- (7) Qin, L., Liu, J., Mills, D. A., Proshlyakov, D. A., Hiser, C., and Ferguson-Miller, S. (2009) Redox-dependent conformational changes in cytochrome *c* oxidase suggest a gating mechanism for proton uptake. *Biochemistry* 48, 5121–5130.
- (8) Zhu, J., Han, H., Pawate, A., and Gennis, R. (2010) Decoupling mutations in the D-channel of the  $aa_3$ -type cytochrome *c* oxidase from *Rhodobacter sphaeroides* suggest that a continuous hydrogen bonded chain of waters is essential for proton pumping. *Biochemistry* 49, 4476–4482.
- (9) Wikstrom, M., Ribacka, C., Molin, M., Laakkonen, L., Verkhovsky, M., and Puustinen, A. (2005) Gating of proton and water transfer in the respiratory enzyme cytochrome *c* oxidase. *Proc. Natl. Acad. Sci. U.S.A.* 102, 10478–10481.
- (10) Seibold, S. A., Mills, D. A., Ferguson-Miller, S., and Cukier, R. I. (2005) Water chain formation and possible proton pumping routes in *Rhodobacter sphaeroides* cytochrome *c* oxidase: A molecular dynamics comparison of the wild type and R481K mutant. *Biochemistry* 44, 10475–10485.
- (11) Kaila, V. R., Sharma, V., and Wikstrom, M. (2011) The identity of the transient proton loading site of the proton-pumping mechanism of cytochrome *c* oxidase. *Biochim. Biophys. Acta* 1807, 80–84.
- (12) Mills, D. A., and Hosler, J. P. (2005) Slow proton transfer through the pathways for pumped protons in cytochrome *c* oxidase induces suicide inactivation of the enzyme. *Biochemistry* 44, 4656–4666.
- (13) Bratton, M. R., Pressler, M. A., and Hosler, J. P. (1999) Suicide inactivation of cytochrome *c* oxidase: Catalytic turnover in the absence of subunit III alters the active site. *Biochemistry* 38, 16236–16245.

- (14) Mills, D. A., Tan, Z., Ferguson-Miller, S., and Hosler, J. (2003) A role for subunit III in proton uptake into the D pathway and a possible proton exit pathway in *Rhodobacter sphaeroides* cytochrome *c* oxidase. *Biochemistry* 42, 7410–7417.
- (15) Varanasi, L., and Hosler, J. P. (2012) Subunit III-depleted cytochrome *c* oxidase provides insight into the process of proton uptake by proteins. *Biochim. Biophys. Acta* 1817, 545–551.
- (16) Gilderson, G., Salomonsson, L., Aagaard, A., Gray, J., Brzezinski, P., and Hosler, J. (2003) Subunit III of cytochrome *c* oxidase of *Rhodobacter sphaeroides* is required to maintain rapid proton uptake through the D pathway at physiologic pH. *Biochemistry* 42, 7400–7409.
- (17) Adelroth, P., and Hosler, J. (2006) Surface proton donors for the D-pathway of cytochrome *c* oxidase in the absence of subunit III. *Biochemistry* 45, 8308–8318.
- (18) Brzezinski, P., and Johansson, A. L. (2010) Variable proton-pumping stoichiometry in structural variants of cytochrome *c* oxidase. *Biochim. Biophys. Acta* 1797, 710–723.
- (19) Johansson, A. L., Carlsson, J., Hogbom, M., Hosler, J. P., Gennis, R. B., and Brzezinski, P. (2013) Proton uptake and pKa changes in the uncoupled Asn139Cys variant of cytochrome *c* oxidase. *Biochemistry* 52, 827–836.
- (20) Johansson, A. L., Hogbom, M., Carlsson, J., Gennis, R. B., and Brzezinski, P. (2013) Role of aspartate 132 at the orifice of a proton pathway in cytochrome *c* oxidase. *Proc. Natl. Acad. Sci. U.S.A.* 110, 8912–8917.
- (21) Sacks, V., Marantz, Y., Aagaard, A., Checover, S., Nachliel, E., and Gutman, M. (1998) The dynamic feature of the proton collecting antenna of a protein surface. *Biochim. Biophys. Acta* 1365, 232–240.
- (22) Kirchberg, K., Michel, H., and Alexiev, U. (2013) Exploring the entrance of proton pathways in cytochrome *c* oxidase from *Paracoccus denitrificans*: Surface charge, buffer capacity and redox-dependent polarity changes at the internal surface. *Biochim. Biophys. Acta* 1827, 276–284.
- (23) Zhen, Y., Qian, J., Follmann, K., Hayward, T., Nilsson, T., Dahn, M., Hilmi, Y., Hamer, A. G., Hosler, J. P., and Ferguson-Miller, S. (1998) Overexpression and purification of cytochrome *c* oxidase from *Rhodobacter sphaeroides*. *Protein Expression Purif.* 13, 326–336.
- (24) Bratton, M., Mills, D., Castleden, C. K., Hosler, J., and Meunier, B. (2003) Disease-related mutations in cytochrome *c* oxidase studied in yeast and bacterial models. *FEBS J.* 270, 1222–1230.
- (25) Hosler, J. P., Fetter, J., Tecklenburg, M. M. J., Espe, M., Lerma, C., and Ferguson-Miller, S. (1992) Cytochrome-*aa*<sub>3</sub> of *Rhodobacter sphaeroides* as a model for mitochondrial cytochrome *c* oxidase: Purification, kinetics, proton pumping, and spectral analysis. *J. Biol. Chem.* 267, 24264–24272.
- (26) Junemann, S., Meunier, B., Gennis, R. B., and Rich, P. R. (1997) Effects of mutation of the conserved lysine-362 in cytochrome *c* oxidase from *Rhodobacter sphaeroides*. *Biochemistry* 36, 14456–14464.
- (27) Cvetkov, T. L., and Prochaska, L. J. (2007) Biophysical and biochemical characterization of reconstituted and purified *Rhodobacter sphaeroides* cytochrome *c* oxidase in phospholipid vesicles sheds insight into its functional oligomeric structure. *Protein Expression Purif.* 56, 189–196.
- (28) Schagger, H., and von Jagow, G. (1991) Blue native electrophoresis for isolation of membrane protein complexes in enzymatically active form. *Anal. Biochem.* 199, 223–231.
- (29) Fuller, S. D., Darleyusmar, V. M., and Capaldi, R. A. (1981) Covalent complex between yeast cytochrome *c* and beef heart cytochrome *c* oxidase which is active in electron transfer. *Biochemistry* 20, 7046–7053.
- (30) van Gelder, B., and Slater, E. C. (1962) The extinction coefficient of cytochrome *c*. *Biochim. Biophys. Acta* 58, 593–595.
- (31) Riegler, D., Shroyer, L., Pokalsky, C., Zaslavsky, D., Gennis, R., and Prochaska, L. J. (2005) Characterization of steady-state activities of cytochrome *c* oxidase at alkaline pH: Mimicking the effect of K-channel mutations in the bovine enzyme. *Biochim. Biophys. Acta* 1706, 126–133.
- (32) Hiser, C., Buhrow, L., Liu, J., Kuhn, L., and Ferguson-Miller, S. (2013) A conserved amphipathic ligand binding region influences K-path-dependent activity of cytochrome *c* oxidase. *Biochemistry* 52, 1385–1396.
- (33) Varanasi, L., and Hosler, J. (2011) Alternative initial proton acceptors for the D pathway of *Rhodobacter sphaeroides* cytochrome *c* oxidase. *Biochemistry* 50, 2820–2828.
- (34) Mills, D. A., and Ferguson-Miller, S. (2002) Influence of structure, pH and membrane potential on proton movement in cytochrome oxidase. *Biochim. Biophys. Acta* 1555, 96–100.
- (35) Qin, L., Mills, D. A., Hiser, C., Murphree, A., Garavito, R. M., Ferguson-Miller, S., and Hosler, J. (2007) Crystallographic location and mutational analysis of Zn and Cd inhibitory sites and role of lipidic carboxylates in rescuing proton path mutants in cytochrome *c* oxidase. *Biochemistry* 46, 6239–6248.
- (36) Aagaard, A., and Brzezinski, P. (2001) Zinc ions inhibit oxidation of cytochrome *c* oxidase by oxygen. *FEBS Lett.* 494, 157–160.
- (37) Francia, F., Giachini, L., Boscherini, F., Venturoli, G., Capitanio, G., Martino, P. L., and Papa, S. (2007) The inhibitory binding site(s) of Zn<sup>2+</sup> in cytochrome *c* oxidase. *FEBS Lett.* 581, 611–616.
- (38) Muramoto, K., Hirata, K., Shinzawa-Itoh, K., Yoko-o, S., Yamashita, E., Aoyama, H., Tsukihara, T., and Yoshikawa, S. (2007) A histidine residue acting as a controlling site for dioxygen reduction and proton pumping by cytochrome *c* oxidase. *Proc. Natl. Acad. Sci. U.S.A.* 104, 7881–7886.
- (39) Konstantinov, A. A., Siletsky, S., Mitchell, D., Kaulen, A., and Gennis, R. B. (1997) The roles of the two proton input channels in cytochrome *c* oxidase from *Rhodobacter sphaeroides* probed by the effects of site-directed mutations on time-resolved electrogenic intraprotein proton transfer. *Proc. Natl. Acad. Sci. U.S.A.* 94, 9085–9090.
- (40) Konstantinov, A. A., Vygodina, T., Capitanio, N., and Papa, S. (1998) Ferrocyanide-peroxidase activity of cytochrome *c* oxidase. *Biochim. Biophys. Acta* 1363, 11–23.
- (41) Vygodina, T. V., Pecoraro, C., Mitchell, D., Gennis, R., and Konstantinov, A. A. (1998) Mechanism of inhibition of electron transfer by amino acid replacement K362M in a proton channel of *Rhodobacter sphaeroides* cytochrome *c* oxidase. *Biochemistry* 37, 3053–3061.
- (42) Verkhovsky, M. I., Morgan, J. E., and Wikstrom, M. (1995) Control of electron delivery to the oxygen reduction site of cytochrome *c* oxidase: A role for protons. *Biochemistry* 34, 7483–7491.
- (43) Karpefors, M., Adelroth, P., Zhen, Y., Ferguson-Miller, S., and Brzezinski, P. (1998) Proton uptake controls electron transfer in cytochrome *c* oxidase. *Proc. Natl. Acad. Sci. U.S.A.* 95, 13606–13611.
- (44) Verkhovsky, M. I., Belevich, I., Bloch, D. A., and Wikstrom, M. (2006) Elementary steps of proton translocation in the catalytic cycle of cytochrome oxidase. *Biochim. Biophys. Acta* 1757, 401–407.
- (45) Vanneste, W. H. (1966) The stoichiometry and absorption spectra of components *a* and *a*<sub>3</sub> in cytochrome *c* oxidase. *Biochemistry* 5, 838–848.
- (46) Prochaska, L. J., and Reynolds, K. A. (1986) Characterization of electron-transfer and proton-translocation activities in bovine heart mitochondrial cytochrome *c* oxidase deficient in subunit III. *Biochemistry* 25, 781–787.
- (47) Prochaska, L. J., and Fink, P. S. (1987) On the role of subunit III in proton translocation in cytochrome *c* oxidase. *J. Bioenerg. Biomembr.* 19, 143–166.
- (48) Wilson, K. S., and Prochaska, L. J. (1990) Phospholipid vesicles containing bovine heart mitochondrial cytochrome *c* oxidase and subunit III-deficient enzyme: Analysis of respiratory control and proton translocating activities. *Arch. Biochem. Biophys.* 282, 413–420.
- (49) Wu, S., Moreno-Sanchez, R., and Rottenberg, H. (1995) Involvement of cytochrome *c* oxidase subunit III in energy coupling. *Biochemistry* 34, 16298–16305.
- (50) Adelroth, P., and Brzezinski, P. (2004) Surface-mediated proton-transfer reactions in membrane-bound proteins. *Biochim. Biophys. Acta* 1655, 102–115.



- (51) Marantz, Y., Einarsdottir, O. O., Nachliel, E., and Gutman, M. (2001) Proton-collecting properties of bovine heart cytochrome *c* oxidase: Kinetic and electrostatic analysis. *Biochemistry* 40, 15086–15097.
- (52) Haltia, T., Semo, N., Arrondo, J. L., Goni, F. M., and Freire, E. (1994) Thermodynamic and structural stability of cytochrome *c* oxidase from *Paracoccus denitrificans*. *Biochemistry* 33, 9731–9740.
- (53) Varanasi, L., Mills, D., Murphree, A., Gray, J., Purser, C., Baker, R., and Hosler, J. (2006) Altering conserved lipid binding sites in cytochrome *c* oxidase of *Rhodobacter sphaeroides* perturbs the interaction between subunits I and III and promotes suicide inactivation of the enzyme. *Biochemistry* 45, 14896–14907.
- (54) Varanasi, L., Mills, D., Murphree, A., Gray, J., Purser, C., Baker, R., and Hosler, J. (2006) Altering conserved lipid binding sites in cytochrome *c* oxidase of *Rhodobacter sphaeroides* perturbs the interaction between subunits I and III and promotes suicide inactivation of the enzyme. *Biochemistry* 45, 14896–14907.
- (55) Marantz, Y., Nachliel, E., Aagaard, A., Brzezinski, P., and Gutman, M. (1998) The proton collecting function of the inner surface of cytochrome *c* oxidase from *Rhodobacter sphaeroides*. *Proc. Natl. Acad. Sci. U.S.A.* 95, 8590–8595.
- (56) Llopis, J., McCaffery, J. M., Miyawaki, A., Farquhar, M. G., and Tsien, R. Y. (1998) Measurement of cytosolic, mitochondrial, and Golgi pH in single living cells with green fluorescent proteins. *Proc. Natl. Acad. Sci. U.S.A.* 95, 6803–6808.
- (57) Rich, P. R., and Marechal, A. (2013) Functions of the hydrophilic channels in protonmotive cytochrome *c* oxidase. *J. R. Soc., Interface* 10, 20130183.
- (58) Distler, A. M., Allison, J., Hiser, C., Qin, L., Hilmi, Y., and Ferguson-Miller, S. (2004) Mass spectrometric detection of protein, lipid and heme components of cytochrome *c* oxidase from *R. sphaeroides* and the stabilization of non-covalent complexes from the enzyme. *Eur. J. Mass Spectrom.* 10, 295–308.